

Optimal synchronization of complex networks

Per Sebastian Skardal,^{1,2,*} Dane Taylor,^{2,3,4,†} and Jie Sun^{5,‡}

¹*Departament d'Enginyeria Informàtica i Matemàtiques, Universitat Rovira i Virgili, 43007 Tarragona, Spain*

²*Department of Applied Mathematics, University of Colorado at Boulder, Colorado 80309, USA*

³*Statistical and Applied Mathematical Sciences Institute, Research Triangle Park, NC 27709, USA*

⁴*Department of Mathematics, University of North Carolina, Chapel Hill, NC 27599, USA*

⁵*Department of Mathematics, Clarkson University, Potsdam, NY 13699, USA*

We study optimal synchronization in networks of heterogeneous phase oscillators. Our main result is the derivation of a *synchrony alignment function* that encodes the interplay between network structure and oscillators' frequencies and can be readily optimized. We highlight its utility in two general problems: constrained frequency allocation and network design. In general, we find that synchronization is promoted by strong alignments between frequencies and the dominant Laplacian eigenvectors, as well as a qualitative matching between the heterogeneity of frequencies and network structure.

PACS numbers: 05.45.Xt, 89.75.Hc

A central goal of complexity theory is to understand the emergence of collective behavior in large ensembles of interacting dynamical systems. Synchronization of network-coupled oscillators has served as a paradigm for understanding the emergence of ordered behavior and self-organization [1–4]. Examples of synchronization can be found in nature, such as the simultaneous flashing of fireflies [5] and cardiac pacemaker cells [6], in engineering, such as the power grid [7] and oscillations of pedestrian bridges [8], and at their intersection, for example, with synthetic cell engineering [9]. We consider here the dynamics of N network-coupled limit cycle oscillators, each described by the phase θ for $i = 1, \dots, N$, whose time evolution is governed by

$$\dot{\theta}_i = \omega_i + K \sum_{j=1}^N A_{ij} H(\theta_j - \theta_i). \quad (1)$$

Here ω_i is the natural frequency of oscillator i , $K > 0$ is the coupling strength, $[A_{ij}]$ is the adjacency matrix of the underlying network, and H is a 2π -periodic coupling function [10]. The choices $H(\theta) = \sin(\theta)$ and $H(\theta) = \sin(\theta - \alpha)$ with the phase-lag parameter $\alpha \in (0, \pi/2)$ yield the classical Kuramoto and Sakaguchi-Kuramoto models, respectively [11, 12]. Here we treat $H(\theta)$ with full generality so long as $H'(\theta) > 0$.

Considerable research has shown that the underlying structure of a network plays a crucial role in determining its synchronizability [13–22]. However, despite the large volume of research in this direction, the precise relationship between the dynamical and structural properties of a network and its synchronization remains not fully understood. One fundamental unanswered question that is of interest to theorists and engineers alike is, given an objective measure of synchronization, how can synchronization be *optimized*? One application lies in synchronizing the power grid [23], where sources and loads can be modeled as oscillators with different frequencies. To this end, we ask the following question: what structural and/or dynamical properties should be present to optimize synchronization?

In this Letter, we measure the degree of synchronization of an ensemble of oscillators using the standard Kuramoto order parameter defined by

$$re^{i\psi} = \frac{1}{N} \sum_{j=1}^N e^{i\theta_j}. \quad (2)$$

Here $re^{i\psi}$ represents the centroid of all phases placed on the complex unit circle, with r being its magnitude. Thus, $r \approx 0$ and $r = 1$ correspond to incoherent and synchronized states, respectively, with intermediate values corresponding to partially synchronized states [11]. In general, the question of how to optimize synchronization (here we consider maximizing r) is challenging due to the fact that the macroscopic system dynamics depend on both the dynamics of individual units (i.e., the natural frequencies) and the structure of the network (i.e., encoded by the adjacency matrix). To quantify the interplay between node dynamics and network structure, we derive directly from Eqs. (1) and (2) a *synchrony alignment function* which serves as an objective measure of synchronization and can be used to systematically optimize the synchronization properties of the network. We highlight the applicability of the synchrony alignment function by addressing two complementary classes of optimization problems. The first is *constrained frequency allocation*, where given a fixed network topology, frequencies must be chosen optimally. The second is *network design*, where given a fixed set of frequencies, an optimal network structure must be found. We introduce both problems generally and note that either can be easily adapted to a wide range of applications by imposing additional constraints. We next present the derivation of the synchrony alignment function. No assumptions are made about the frequencies or network structure aside from the network being connected and undirected, and thus we consider a general frequency vector $\omega = [\omega_1, \dots, \omega_N]^T$ and adjacency matrix A .

We begin by considering the dynamics of Eq. (1) in the strong coupling regime where $r \approx 1$. In this regime the oscillators are entrained in a tight cluster such that $\theta_i \approx \theta_j$ for all

(i, j) pairs, so that expanding Eq. (1) yields

$$\dot{\theta}_i \approx \tilde{\omega}_i - K \sum_{j=1}^N L_{ij} \theta_j, \quad (3)$$

where $\tilde{\omega}_i = \omega_i + KH(0)d_i$, $d_i = \sum_{j=1}^N A_{ij}$ is the degree of node i , and $[L_{ij}]$ is the Laplacian matrix whose entries are defined as $L_{ij} = \delta_{ij}d_i - (1 - \delta_{ij})A_{ij}$.

The spectral properties of the Laplacian are essential to our analysis, so we summarize them here. First, since the network is connected and undirected, all the eigenvalues of L are real and can be ordered as $0 = \lambda_1 < \lambda_2 \leq \dots \leq \lambda_{N-1} \leq \lambda_N$. Second, after normalization, the eigenvectors $\{\mathbf{v}^i\}_{i=1}^N$ form an orthonormal basis for \mathbb{R}^N . Furthermore, the eigenvector associated with $\lambda_1 = 0$ is $\mathbf{v}^1 = \mathbf{1}$, which corresponds to the synchronization manifold. Nonetheless, $\{\mathbf{v}^i\}_{i=1}^N$ is an orthonormal basis of \mathbb{R}^N .

Inspecting Eq. (3) and entering the rotating reference frame $\theta_i \mapsto \theta_i + \Omega t$ where $\tilde{\Omega} = \langle \omega \rangle + KH(0)\langle d \rangle$, we find that if a steady-state solution θ^* exists, it is given by

$$\theta^* = L^\dagger \tilde{\omega} / KH'(0), \quad (4)$$

where $L^\dagger = \sum_{j=2}^N \lambda_j^{-1} \mathbf{v}^j \mathbf{v}^{jT}$ is the pseudo-inverse of L [24]. We next consider the order parameter for such a steady-state solution θ^* . First, with a suitable shift in initial conditions the average phase can be set to zero, implying that the sum on the right-hand-side of Eq. (2) is real. Furthermore, in the strongly synchronized regime all phases are tightly packed about $\psi = 0$, thus $|\theta_j^*| \ll 1$ for all n . Expanding Eq. (2) yields

$$r \approx 1 - \|\theta^*\|^2 / 2N. \quad (5)$$

Finally, we use the definition of the pseudo-inverse, take the norm of Eq. (4), and insert this into Eq. (5) to obtain

$$r = 1 - J(\tilde{\omega}, L) / 2K^2 H'^2(0), \quad (6)$$

for which we define the synchrony alignment function

$$J(\tilde{\omega}, L) = \frac{1}{N} \sum_{j=2}^N \lambda_j^{-2} \langle \mathbf{v}^j, \tilde{\omega} \rangle^2. \quad (7)$$

The derivation of $J(\tilde{\omega}, L)$ is our main theoretical result as its minimization corresponds to the maximization of the order parameter r , which allows for the optimization of synchronization using elementary properties of the network (i.e., Laplacian eigenvalues and eigenvectors) and the oscillators (i.e., the frequency vector). Before exploring the optimization of $J(\tilde{\omega}, L)$, we point out a few interesting and somewhat unexpected results. On the one hand, for coupling functions with $H(0) = 0$ [such as the Kuramoto model with $H(\theta) = \sin(\theta)$], it follows that $\tilde{\omega} = \omega$, and thus optimization of $J(\tilde{\omega}, L)$ is independent of K . On the other hand, when $H(0) \neq 0$, in the limit $K \rightarrow \infty$, Eq. (6) yields $r = 1 - J(\mathbf{d}, L)H^2(0)/2H'^2(0)$,

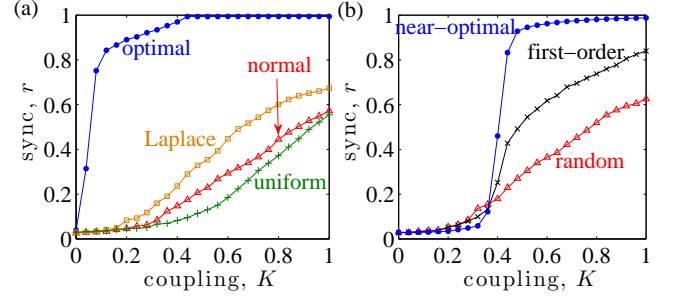


FIG. 1. (Color online) Constrained frequency allocation: (a) r vs K for optimal allocation (blue circles) compared with random allocations drawn from normal (red triangles), uniform (green pluses), and Laplace (orange squares) distributions. (b) r vs K for a pre-chosen set of normally distributed frequencies with random (red triangles), first-order (black crosses), and near optimal (blue circles) arrangements. The near optimal arrangement was obtained from $S = 10^6$ proposed frequency exchanges. Networks are SF with $N = 1000$, $\gamma = 3$, and $d_0 = 2$.

implying that perfect synchrony, i.e., $r = 1$ is not attainable. It follows that the existence of a strong coupling regime $r \lesssim 1$ and consequently the approximations in our theory are valid only when $J(\mathbf{d}, L)H^2(0)/2H'^2(0) \ll 1$. Furthermore, since $\tilde{\omega}$ depends on the coupling strength K , so will the optimization of $J(\tilde{\omega}, L)$ and therefore the optimal network. From now on, we will specialize to the widely used Kuramoto model, $H(\theta) = \sin(\theta)$, although we emphasize that similar results as those that follow can be obtained for more general coupling functions, e.g., the Sakaguchi-Kuramoto model. We will highlight the utility of the synchrony alignment function for two classes of optimization problem: constrained frequency allocation and optimal network design.

We first address constrained frequency allocation for a fixed network. We note that by entering a rotating frame we can without any loss of generality set the mean frequency $\langle \omega \rangle$ to zero. Furthermore, without constraining ω , the choice of $\omega = [0, \dots, 0]^T$ trivially minimizes Eq. (7), resulting in $r = 1$, so we require as a first constraint that ω has a fixed standard deviation, $\sigma = \sqrt{N^{-1} \sum_i \omega_i^2}$. By rescaling time and the coupling strength, σ can be tuned freely, so without any loss of generality we set $\sigma = 1$. To minimize $J(\omega, L)$, we first express ω as a linear combination of the nontrivial eigenvectors of L , $\omega = \sum_{i=2}^N \alpha_i \mathbf{v}^i$, where the coefficients must satisfy $\sum_{i=2}^N \alpha_i^2 = N$. After inserting this representation of ω into Eq. (7) it follows that $J(\omega, L)$ is minimized precisely by the choice $\alpha_2, \dots, \alpha_{N-1} = 0$ and $\alpha_N = \sqrt{N}$, yielding $r = 1 - 1/2\lambda_N^2 K^2$. Physically, this corresponds to aligning ω with the dominant eigenvector \mathbf{v}^N .

In Fig. 1 (a) we compare the results of optimal allocation, $\omega = \sqrt{N} \mathbf{v}^N$, with several random frequency allocations by plotting the synchrony profiles r vs K for the optimal allocation, and those for frequencies randomly drawn from normal, uniform, and Laplace distribution (each with unit standard deviation). The underlying network with $N = 1000$ nodes was constructed using the configuration model [25]

with a scale-free (SF) degree distribution $P(d) \propto d^{-\gamma}$ for $\gamma = 3$ and minimum degree $d_0 = 2$. The optimal allocation shows a large improvement over all random alignments and is marked by a sharp transition to a strongly synchronized state at a very small coupling strength, while random allocations produce very gradual transitions. We note that two mechanisms contribute to the excellent performance of the optimal allocation: the choice of frequencies and the nodes to which they are assigned.

The next experiment elucidates the roles these two mechanisms play in optimizing synchronization by considering an additional constraint where frequencies $\{\omega_i\}_{i=1}^N$ are pre-chosen and must be arranged optimally on the network to minimize $J(\omega, L)$. Finding the global minimum requires an exhaustive search over all $N!$ possible arrangements of ω —an unrealistic option even for moderately sized networks. We therefore provide two alternatives: a *first-order* approximation applicable for networks in which the largest Laplacian eigenvalue λ_N is well separated from the others (which is often the case for real world networks including those with scale-free degree distributions [26]) and a *near-optimal* solution based on an accept/reject algorithm. In particular, when the dominant eigenvalue is well separated, $\lambda_i \ll \lambda_N$ for $i \neq N$, an inexpensive first-order minimization of the objective function leads to maximizing $|\langle v^N, \omega \rangle|$. This can be done simply by finding the index permutations i_1, \dots, i_N and j_1, \dots, j_N that place eigenvector entries in ascending order, $v_{i_1}^N \leq \dots \leq v_{i_N}^N$, and frequencies in ascending (or descending) order, $\omega_{j_1} \leq \dots \leq \omega_{j_N}$ (or $\omega_{j_1} \geq \dots \geq \omega_{j_N}$). In principle both pairings must be checked to select the best result, but typically yield comparable results. To find the near-optimal arrangement we begin with an initial arrangement ω and construct a new arrangement ω' by exchanging two randomly chosen entries. If $J(\omega', L) < J(\omega, L)$ we accept ω' , otherwise we reject it. This procedure is then repeated for S proposed exchanges.

In Fig. 1 (b) we compare synchronization profiles for the near-optimal and first-order arrangements to a random placement of frequencies drawn from the unit normal distribution. As expected, the near-optimal arrangement yields the best results, however, the first-order arrangement also performs well, providing an inexpensive way to improve upon purely random arrangements. These results also allow us to compare the potential of arranging pre-chosen frequencies and choosing frequencies freely under the constraint of a set standard deviation [recall Fig. 1 (a)]. In both cases, the transition from incoherence to strong synchronization is very sharp, however it occurs at a larger coupling strength ($K \approx 0.4$) when frequencies are pre-chosen, yielding two distinct regimes: for small K strong synchronization is only attainable when frequencies are freely tunable, while for larger K strong synchronization is attainable even when the frequency set is fixed.

Next we address the complimentary problem of constrained frequency allocation: optimal network design for a fixed set of frequencies. Given ω , we look for a network that minimizes $J(\omega, L)$ for an undirected, unweighted network with a pre-

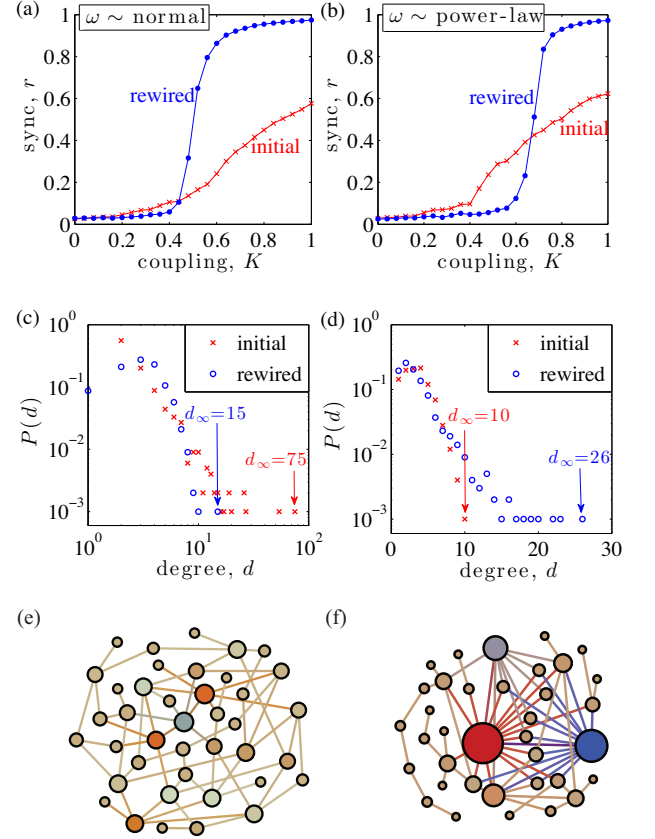


FIG. 2. (Color online) Network design: (a)-(b) r vs K for initial (red crosses) and rewired (blue circles) networks with normal and power-law distributed frequencies. (c)-(d) Degree distributions of the initial (red crosses) and rewired (blue circles) networks. (e)-(f) Illustrations for $N = 40$ and 36 of networks after rewiring.

scribed number of links. As an algorithmic method for obtaining an approximate solution, we initialize an accept/reject algorithm with a network satisfying these constraints, and allow it to evolve as follows. A new network with Laplacian matrix L' is constructed by randomly deleting a link and introducing another between two previously disconnected nodes. If $J(\omega, L') < J(\omega, L)$ we accept the new network, otherwise we reject it. This procedure is then repeated for S proposed rewirings. In Fig. 2 we present the results of this rewiring algorithm for two experiments. We consider two networks: one with relatively homogeneous frequencies drawn from a unit normal distribution (left column) and a second with heterogeneous frequencies drawn from a symmetric power-law distribution, $g(|\omega|) \sim |\omega|^{-3}$ (right column). Both networks contain $N = 1000$ oscillators. In Figs. 2 (a) and (b) we plot the synchronization profiles for the initial networks and the networks obtained after $2 \cdot 10^4$ rewirings. In both experiments, the rewired networks display better synchronization properties with sharp transitions from incoherence to strong synchronization regime. To highlight the adaptability of the synchrony alignment function, each experiment is initialized with a different network topology: a SF network constructed by the configuration model with $\gamma = 3$ and $d_0 = 2$ and an Erdős-

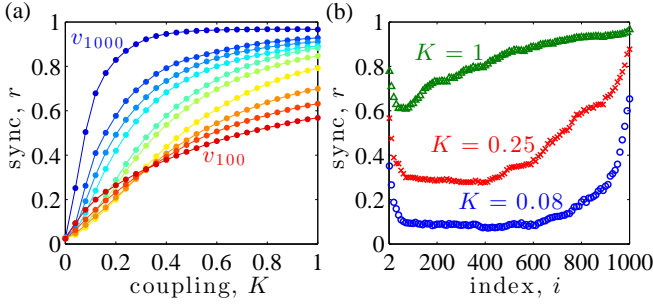


FIG. 3. (Color online) Eigenvector alignments: (a) r vs K for frequency alignments $\omega \propto v^{100}, v^{200}, \dots, v^{1000}$ (red to blue). (b) r vs eigenvector index i for $\omega \propto v^i$ with fixed $K = 0.08$ (blue circles), 0.25 (red crosses), and 1 (green triangles). Each point is averaged over 50 SF network realization of size $N = 1000$ with $\gamma = 3$ and $d_0 = 2$.

Rényi (ER) [27] network with average degree $\langle d \rangle = 4$ are paired with the normally and power-law distributed frequencies, respectively. In Figs. 2 (c) and (d) we plot the initial and rewired degree distributions. In both experiments the degree distribution evolves to better match that of the frequencies, either becoming less [Fig. 2(c)] or more [Fig. 2(d)] heterogeneous. This is further emphasized by the shifts in the maximal degrees d_∞ , which decreases from 75 to 15 for the normally distributed frequencies and increases from 10 to 26 for the power-law distributed frequencies. This suggests that for non-identical oscillators, a more heterogeneous network better synchronizes a more heterogeneous set of frequencies. To illustrate this phenomenon, we show in Figs. 2 (e) and (f) networks resulting from the same experiment with fewer nodes ($N = 40$ and 36 , respectively). Each node is drawn with a radius proportional to its degree and positive (negative) frequencies are colored red (blue). Here the phenomenon is easily observable with the emergence of a few network hubs in (f) but not (e). Also note that the hubs in (f) correspond to those oscillators with the largest frequencies in magnitude, suggesting the existence of a correlation between the frequency and degree, which we discuss in more detail below.

We now study in more detail the synchrony alignment function given in Eq. (7). Just as aligning ω with v^N maximizes r , it follows that in the strong coupling regime, aligning ω with other eigenvectors v^i of decreasing index yields weaker synchronization. We consider the alignments $\omega \propto v^i$ and plot the synchronization profiles in Fig. 3 (a) for $i = 100, 200, \dots, 1000$ (red to blue) averaged over 50 realizations of SF networks with parameters $N = 1000$, $\gamma = 3$, and $d_0 = 2$. As expected, we observe weaker synchronization with decreasing index. We also plot in panel (b) r vs the index value i for a few isolated coupling strengths: $K = 0.08$, 0.25 , and 1 , again averaged over 50 realizations. For all three coupling strengths r tends to increase with i , provided i is not too small. For $K = 0.08$ the majority of alignments yield incoherence with r undergoing a sharp increase only near the most dominant eigenvectors, while the increase in r is more gradual for $K = 0.25$ and 1 . We also point out that for very

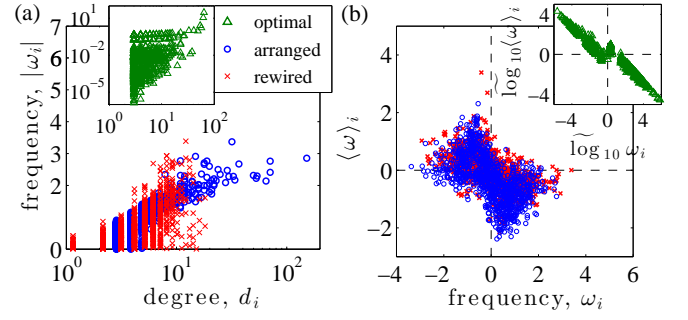


FIG. 4. (Color online) Correlations in synchrony-optimized networks: (a) Frequency magnitude $|\omega_i|$ vs degree d_i and (b) average neighbor frequency $\langle \omega_i \rangle$ vs frequency ω_i for networks with optimally chosen frequencies (green triangles), optimally arranged frequencies (blue circles), and an optimally rewired network (red crosses). Networks are SF with $N = 1000$, $\gamma = 3$, and $d_0 = 3$. Frequencies for the arranged and rewired cases are normally distributed.

small i we observe a short increase in r , which we attribute to local synchronization of different clusters in the network that yield large fluctuations in r .

Before concluding, we investigate the dynamical and structural properties present in optimized networks. In particular, we consider the local degree-frequency and neighboring frequency-frequency correlations that emerge. In Fig. 4 (a) we plot the frequency magnitude $|\omega_i|$ vs degree d_i for synchrony-optimized systems obtained from three methods: optimally chosen frequencies for a fixed network, optimally arranged frequencies for a fixed network, and an optimally rewired network for a fixed frequency vector, each with SF networks with $N = 1000$, $\gamma = 3$, and $d_0 = 3$ and normally-distributed frequencies for the arranged and rewired networks. In each case we observe a strong trend indicating a positive degree-frequency correlation, indicating that the largest frequencies correspond to the network hubs. Moreover, in Fig. 4 (b) we plot for each node i the average frequency of its neighboring oscillators, denoted $\langle \omega \rangle_i = \sum_{j=1}^N A_{ij} \omega_j / d_i$, vs the frequency ω_i . Correlations for the optimal choice (inset) are plotted using $\widetilde{\log_{10} \omega} = \text{sgn}(\omega) \log_{10} |\omega|$ for easier visualization. The results are qualitatively similar for each case, showing a strong negative correlation between frequencies of network neighbors, indicating that, on average, the frequencies of neighboring oscillators are dissimilar. These observations agree with those of Refs. [28, 29], where similar positive and negative correlations were found to promote global synchronization. We finally note that such degree-frequency correlations may help explain the increased abruptness of transitions shown in Figs. 1 and 2 (a) and (b), since similar correlations can lead to discontinuous transitions and other effects [19, 22] (although we did not observe such explosive synchronization here).

In this Letter we have investigated the optimization of network synchronization. Our main result is the derivation of a synchrony alignment function that encodes the interplay between network structure and oscillators' frequencies and allows for a systematic optimization of synchronization. In particular, the synchrony alignment function, which is applica-

ble to a wide range of coupling functions, depends on both the oscillators' frequencies and the network structure via the eigenvalues and eigenvectors of the network Laplacian, making it adaptable to a wide variety of optimization problems. We have demonstrated the power and utility of the synchrony alignment function in two complementary problems for the illustrative case of Kuramoto coupling. First, we considered constrained frequency allocation, where we found that synchronization is promoted by a strong alignment of the frequency vector with the most dominant Laplacian eigenvectors. Second, we considered network design, where we found that, relatively speaking, homogenous networks best synchronize homogenous frequencies, while heterogeneous networks best synchronize heterogeneous frequencies. In all cases we found that in optimized networks the large frequencies are localized to hubs and frequencies of neighboring oscillators are negatively correlated.

Finally, we contrast our results addressing heterogeneous oscillators to the well-developed theory addressing identical oscillators [30]. The synchronizability of a network with identical oscillators is a well-developed concept and can be described entirely by the ratio λ_N/λ_2 of network Laplacian eigenvalues [31], allowing for the optimization of network structure that maximizes synchronizability [32] independent of detailed dynamics. In contrast, we find here that the synchronization of a network of heterogeneous oscillators generally depends on not only the full set of eigenvalues and eigenvectors of the network Laplacian, much like the case of nearly-identical oscillators [33] and oscillators in real-world experiments [34], but more importantly, how the network structure pairs with the heterogeneity of node dynamics (here oscillator frequencies). This suggests that a network that is easily synchronizable with identical oscillators but may have poor synchronization properties with heterogeneous oscillators, and vice-versa.

This work was funded in part by the James S. McDonnell Foundation (PSS), NSF Grant No. DMS-1127914 through the Statistical and Applied Mathematical Sciences Institute (DT), and ARO Grant No. 61386-EG (JS). We thank the referees for their constructive comments, in particular for suggesting the generalization from Kuramoto to arbitrary 2π -periodic coupling functions.

* skardals@gmail.com

† dane.r.taylor@gmail.com

‡ sunj@clarkson.edu

- [1] S. H. Strogatz, *Sync: the Emerging Science of Spontaneous Order* (Hyperion, 2003).
- [2] A. Pikovsky, M. Rosenblum, and J. Kurths, *Synchronization: A Universal Concept in Nonlinear Sciences* (Cambridge University Press, 2003).
- [3] S. N. Dorogovtsev, A. V. Goltsev, and J. F. F. Mendes, *Rev. Mod. Phys.* **80**, 1275 (2008).
- [4] A. Arenas, A. Díaz-Guilera, J. Kurths, Y. Moreno, and C. Zhou, *Phys. Rep.* **469**, 93 (2008).
- [5] J. Buck, *Q. Rev. Biol.* **63**, 265 (1988).
- [6] L. Glass and M. C. Mackey, *From Clocks to Chaos: The Rhythms of Life* (Princeton University Press, Princeton, 1988).
- [7] A. E. Motter, S. A. Myers, M. Anghel, and T. Nishikawa, *Nat. Phys.* **9**, 191 (2013).
- [8] S. H. Strogatz, D. M. Abrams, A. McRobie, B. Eckhardt, and E. Ott, *Nature (London)* **438**, 43 (2005).
- [9] A. Prindle, P. Samayoa, I. Razinkov, T. Danino, L. S. Tsimring, and J. Hasty, *Nature* **481**, 39 (2012).
- [10] H. Daido, *Prog. Theor. Phys.* **88**, 1213 (1992).
- [11] Y. Kuramoto, *Chemical Oscillations, Waves, and Turbulence* (Springer, New York, 1984).
- [12] H. Sakaguchi and Y. Kuramoto, *Prog. Theor. Phys.* **76**, 576 (1986).
- [13] Y. Moreno and A. F. Pacheco, *Europhys. Lett.* **68**, 603 (2004).
- [14] T. Ichinomiya, *Phys. Rev. E* **70** 026116 (2004).
- [15] J. G. Restrepo, E. Ott, and B. R. Hunt, *Phys. Rev. E* **71**, 036151 (2005).
- [16] A. Arenas, A. Díaz-Guilera, and C. J. Pérez-Vicente, *Phys. Rev. Lett.* **96**, 114102 (2006).
- [17] J. Gómez-Gardeñes, Y. Moreno, and A. Arenas, *Phys. Rev. Lett.* **98**, 034101 (2007).
- [18] J. G. Restrepo, E. Ott, and B. R. Hunt, *Phys. Rev. E* **76**, 056119 (2007).
- [19] J. Gómez-Gardeñes, S. Gómez, A. Arenas, and Y. Moreno, *Phys. Rev. Lett.* **106** 128701 (2011).
- [20] P. S. Skardal and J. G. Restrepo, *Phys. Rev. E* **85**, 016208 (2012).
- [21] P. S. Skardal and J. G. Restrepo, *Proceedings of the 2012 International Symposium on Nonlinear Theory and its Applications*, October 22-26, 2012, Palma, Mallorca, Spain.
- [22] P. S. Skardal, J. Sun, D. Taylor, and J. G. Restrepo, *Europhys. Lett.* **101**, 20001 (2013).
- [23] F. Dörfler, M. Chertkov, and F. Bullo, *Proc. Natl. Acad. Sci.* **110**, 2005 (2013).
- [24] A. Ben-Israel and T. N. E. Grenville, *Generalized Inverses* (Springer, New York, 1974).
- [25] A. Békessy, P. Békessy, and J. Komlos, *Stud. Sci. Math. Hung.* **7**, 343 (1972).
- [26] I. J. Farkas, I. Derényi, A.-L. Barabási, and T. Vicsek, *Phys. Rev. E* **64**, 026704 (2001).
- [27] P. Erdős and A. Rényi, *Pub. Math. Inst. Hung. Acad. Sci.* **5**, 17 (1960).
- [28] M. Brede, *Phys. Lett. A* **372**, 2618 (2008).
- [29] L. Buzna, S. Lozano, and A. Díaz-Guilera, *Phys. Rev. E* **80**, 066120 (2009).
- [30] L. M. Pecora and T. L. Carroll, *Phys. Rev. Lett.* **80**, 2109 (1998).
- [31] M. Barahona and L. M. Pecora, *Phys. Rev. Lett.* **89**, 054101 (2002).
- [32] T. Nishikawa and A. E. Motter, *Proc. Natl. Acad. Sci. U.S.A.* **107**, 10 342 (2010).
- [33] J. Sun, E. M. Bollt, and T. Nishikawa, *Europhys. Lett.* **85**, 60011 (2009).
- [34] B. Ravoori, A. B. Cohen, J. Sun, A. E. Motter, T. E. Murphy, and R. Roy, *Phys. Rev. Lett.* **107**, 034102 (2011).